Heliyon 9 (2023) e20629

Contents lists available at ScienceDirect

Heliyon

journal homepage: www.cell.com/heliyon

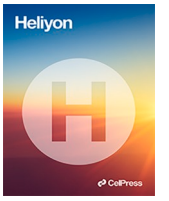

Acidification-based direct electrolysis of treated wastewater for hydrogen production and water reuse

Ji-Hyung Han [a,1,*], Jeongwook Bae [b,c], Joohyun Lim [b,c,1,**], Eunjin Jwa [a], Joo-Youn Nam [a], Kyo Sik Hwang [a], Namjo Jeong [a], Jiyeon Choi [a], Hanki Kim [a], Youn-Cheul Jeung [a]

[a] *Jeju Global Research Centre, Korea Institute of Energy Research, 200 Haemajihaean-ro, Gujwa-eup, Jeju 63357, Republic of Korea*
[b] *Department of Chemistry, Institute for Molecular Science and Fusion Technology, Kangwon National University, Chuncheon, Gangwon, 24341, Republic of Korea*
[c] *Department of Chemistry, Institute for Molecular Science and Fusion Technology, Multidimensional Genomics Research Center, Kangwon National University, Chuncheon, Gangwon, 24341, Republic of Korea*

A R T I C L E I N F O

Keywords:
Treated wastewater
Seawater
Acidification
Bipolar membrane
Inorganic precipitation
Low-grade water electrolysis

A B S T R A C T

This report describes the direct electrolysis of treated wastewater (as a catholyte) to produce hydrogen and potentially reuse the water. To suppress the negative shift of the cathodic potential due to an increase in pH by the hydrogen evolution reaction (HER), the treated wastewater is acidified using the synergetic effect of protons generated from the bipolar membrane and inorganic precipitation occurred at the surface of the cathode during the HER. Natural seawater, as an accessible source for Mg^{2+} ions, was added to the treated wastewater because the concentration of Mg^{2+} ions contained in the original wastewater was too low for acidification to occur. The mixture of treated wastewater with seawater was acidified to pH 3, allowing the initial cathode potential to be maintained for more than 100 h. The amount of inorganic precipitates formed on the cathode surface is greater than that in the control case (adding 0.5 M NaCl instead of seawater) but does not adversely affect the cathodic potential and Faradaic efficiency for H_2 production. Additionally, it was confirmed that less organic matter was adsorbed to the inorganic deposits under acidic conditions. These indicate that acidification plays an important role in improving the performance and stability of low-grade water electrolysis. Considering that the treated wastewater is discharged near the ocean, acidification-based electrolysis of the effluent with seawater can be a water reuse technology for green hydrogen production, enhancing water resilience and contributing to the circular economy of water resources.

* Corresponding author.
** Corresponding author. Department of Chemistry, Institute for Molecular Science and Fusion Technology, Kangwon National University, Chuncheon, Gangwon, 24341, Republic of Korea. Tel.: +82 33 250 848; Fax: +82 33 259 5667.
E-mail addresses: jihyung0760@kier.re.kr (J.-H. Han), jlim@kangwon.ac.kr (J. Lim).
[1] The two authors have the same contribution to this study.

https://doi.org/10.1016/j.heliyon.2023.e20629
Received 23 May 2023; Received in revised form 21 September 2023; Accepted 3 October 2023
Available online 5 October 2023

1. Introduction

Hydrogen is in the spotlight as an energy carrier that can store renewable energy with large output fluctuations and maintain a balance between supply and demand. As hydrogen plays a key role in responding to climate change, developments in hydrogen production technology are actively underway to obtain a hydrogen dependent economy and society. Water electrolysis is an electrochemical method that can produce green hydrogen without carbon emissions when combined with renewable energy. Alkaline water electrolysis and proton exchange membrane water electrolysis have attained the highest technological maturity. They utilize ultrapure water or 20–30 % KOH solution as the electrolyte [1,2]. As the cost of renewable electricity has drastically fallen, the question whether there will be enough water for water electrolysis has been raised [3]. Accessible freshwater accounts for less than 1 % of the water on the planet [4]; therefore, water electrolysis should not place an additional burden on freshwater use, especially in areas where drinking water is difficult to obtain.

Treated wastewater is an important water resource that has not been widely used until now. The amount of domestic and municipal wastewater produced worldwide is estimated at 360 km^3/year, out of which 52 % is treated in wastewater treatment plants [5]. Approximately 10 % of the treated wastewater is currently reused, which is low; however, in a situation where energy consumption continues to increase along with the increasing global water shortage due to climate change, the vitalization of the wastewater reuse market is required [6–8]. Reuse of treated wastewater for various purposes rather than discharging it into the sea can reduce tap water consumption. Although it is proposed to utilize the treated wastewater as an alternative water resource, such as for use as industrial water, agricultural water, and cleaning water, the domestic reuse rate in Korea is very low at approximately 14 %. This is because water quality and aesthetic rejection are primary concerns, which indicates that it is necessary to diversify the types of reuse. Herein, we suggest direct electrolysis of treated wastewater for hydrogen production as a water reuse technology. Low-grade water electrolysis can reduce investment and operating costs for the ultra-purification of treated wastewater, implying that environmental friendliness can be maximized by minimizing the industrial waste generated in the process. The treated wastewater has a considerably lower concentration of organic matter and electrochemically active chemical species than that in the original wastewater. Therefore, hydrogen production efficiency could be effectively maintained without the side reactions, and electrode fouling caused by organic matter can be suppressed.

When the treated wastewater containing various ions is used as a catholyte, the pH increases because of the hydrogen evolution reaction (HER), and consequent inorganic precipitation deteriorates the performance and long-term stability of water electrolysis. The HER driven by the electroreduction of water molecules generates hydroxide anions as a by-product (HER: $2H_2O + 2e^- \rightarrow H_2 + 2OH^-$, $E^0 = -0.828$ V under basic conditions). As the cathode surface becomes more basic during electrolysis, the equilibrium potential of the HER shifts negatively, requiring more electric energy consumption. The alkalization of the catholyte results in the formation of inorganic precipitates [9,10], such as brucite $Mg(OH)_2$ and calcite ($CaCO_3$), through chemical reactions with multivalent cations, such as Mg^{2+} and Ca^{2+} contained in the treated wastewater. Inorganic scaling reduces the number of active sites of electrocatalysts and increases the internal resistance of the electrolyzer, resulting in an increased energy consumption [11–14]. Lu et al. reported that inorganic precipitates formed on the cathode decreased the current density by 50 % within a few hours [15]. Additionally, the alkalized catholyte induces the formation of dispersed inorganic deposits, which easily clog the channels in a large-scale electrolyzer.

Recently, we confirmed that natural seawater, as a catholyte, was acidified to pH 3 during the HER when a bipolar membrane (BPM) was used as a separator [16,17]. The BPM consists of a cation exchange layer (CEL), an anion exchange layer (AEL), and catalysts in the interfacial layer. In a BPM, under reverse-bias conditions, water dissociation (WD: $H_2O \rightarrow H^+ + OH^-$) occurs, which provides protons to the catholyte. The proton flux cooperates with inorganic precipitation capturing OH^- generated from the HER, acidifying seawater. It should be noted that acidification occurs only when inorganic precipitation occurs at the cathode under the reverse bias of the BPM. The acidification of seawater reduces the overpotential for HER and suppresses the formation of dispersed inorganic deposits. The approach used herein is applicable to low-grade water electrolysis utilizing treated wastewater as a catholyte.

In this study, a certain amount of natural seawater was added to the treated wastewater to induce acidification because the concentration of Mg^{2+} ions in the raw wastewater was too low to induce inorganic precipitation. Seawater also serves as a supporting electrolyte because of its high ionic conductivity [18,19]. It was confirmed that the acidification of the treated wastewater maintained the initial cathode potential (E_c) for HER for up to 100 h despite the formation of inorganic precipitates on the surface of the cathode. On the other hand, in the control case (with 0.5 M NaCl instead of seawater), the treated wastewater was alkalized, showing a large increase in E_c (~200 mV). More inorganic precipitates were formed on the cathode under acidic conditions owing to the addition of seawater, whereas more organic matter contained in the treated wastewater adsorbed to the inorganic deposits under alkaline conditions. We also analyzed changes in the properties of the treated wastewater before and after electrolysis.

2. Experimental

2.1. Characteristics of treated wastewater and natural seawater

The treated wastewater was obtained from Jeju sewage treatment plants. The legal standards for effluent quality in the Republic of Korea are as follows: BOD (Biochemical Oxygen Demand) < 10 ppm, COD (Chemical Oxygen Demand) < 40 ppm, SS (Suspended Solid) < 10 ppm, T-N (Total Nitrogen) < 20 ppm, and T-P (Total Phosphorous) < 0.5 ppm. Natural seawater was collected from the sea near the institute. The treated wastewater and seawater were stored at a temperature of approximately 5 °C to prevent biodegradation due to microbial action. The compositions of the treated wastewater and seawater were analyzed using a total organic carbon analyzer

(TOC-L, Shimadzu, Japan) and inductively coupled plasma optical emission spectroscopy (ICP-OES, AVIO 500, PerkinElmer, USA). The characteristics are listed in Table 1.

2.2. Batch-typed low-grade water electrolyzer with zero-gap configuration

A batch-type cell, as described in a previous paper [16], consisting of two chambers (acryl, internal dimensions: $5 \times 5 \times 5$ cm^3) with a BPM (as a separator, Astom Corp. Japan) was used for low-grade water electrolysis. Each chamber contained 120 mL of electrolyte. The effective area of the BPM (7.065 cm^2) was identical to the geometrical area of the electrode in contact with the electrolyte. Porous electrodes are composed of titanium (Ti) fibers, resulting in pores of hundreds of micrometers [17]. Ti fibers (Bekaert, Japan, dia. 20 μm, weight: 400 g/m^2, porosity: 78 %, thickness: 400 μm) were coated with Ru/Ir and Ir as cathode and anode, respectively. The roughness factor (ratio of the real surface area to the geometrical area) of the porous electrode was approximately 70 [17].

A zero gap between the electrode and BPM was applied to minimize the bubble resistance. A mixture of treated wastewater (130 mL) and natural seawater (70 mL) was directly used as the catholyte without filtration or purification. For the control experiment, 0.5 M NaCl (70 mL) was added to the treated wastewater to achieve a similar ionic conductivity. NaOH solution (0.5 M) was used as the anolyte to achieve a highly selective oxygen evolution reaction (OER: $4OH^- \rightarrow O_2 + 2H_2O + 4e^-, E^0 = 0.401\ V$) based on the greatest differences in the standard potential of the OER and chlorine evolution reaction (ClER) under alkaline conditions [20].

2.3. Electrochemical characterization

Electrochemical experiments were performed at room temperature (25 °C) using a potentiostat (ZIVE MP2C, WonaTech, Republic of Korea). During the chronopotentiometric measurement of the cell potential (E_{cell}) at 20 mA/cm^2 (normalized to the geometrical area of the electrode), the cathode potential (E_c) and anode potential (E_a) were monitored against an Ag/AgCl reference electrode using an auxiliary connection. The membrane potential (E_m) across the BPM was measured using two reference electrodes (Fig. S1). To avoid a significant overpotential for water dissociation (WD) in the BPM, a current density of 20 mA/cm^2 was chosen with an E_m of ~0.9 V, which is slightly greater than the thermodynamical potential for WD (~0.83 V). The pH and ionic conductivity of the catholytes were measured at regular intervals (Seven Go Duo SG78, Mettler-Toledo GmbH, Switzerland). The gas produced in each chamber was collected in a gas bag (50 mL, Dalian Delin Gas Packing Co., Ltd., China) during the constant-current experiment for a certain period. The bag was then connected to a gas chromatograph (GC 2014, Shimadzu, Japan) to evaluate the gas components and amounts of hydrogen and oxygen.

2.4. Physical and chemical characterization

The concentration of Mg^{2+} in the treated wastewater before and after 100 h of electrolysis was measured using ion chromatography (ICS-3000, Dionex, USA). A total organic carbon analyzer (TOC-L, Shimadzu, Japan) was used to analyze the dissolved organic carbon in the treated wastewater; samples were filtered using a Whatman 0.45 μm PVDF filters. Acidification, which is a general sample pretreatment to remove inorganic carbon (IC), was not performed to confirm the effect of the catholyte type (or change in catholyte pH) on the total organic carbon (TOC), total nitrogen (TN), IC, and total carbon (TC). Each sample was measured up to three times and the average value was reported as the final result. Porous cathodes with inorganic deposits were analyzed using field-emission scanning electron microscopy (FE-SEM; S-4800, Hitachi, Japan) coupled with quantitative energy-dispersive X-ray spectroscopy (EDX; XMAX 50, Horiba, Japan), X-ray photoelectron spectroscopy (XPS; Nexsa G2, Thermo Scientific, USA), and X-ray diffraction (XRD; SmartLab high-resolution, Rigaku, Japan).

2.5. Calculation of faradaic efficiency

The Faradaic efficiency was calculated as the experimental moles of hydrogen or oxygen divided by the theoretical value.

$$\text{Faradaic efficiency} = \frac{experimental\ moles}{theoretical\ moles} \times 100 \quad (1)$$

Table 1
Characteristics of the treated wastewater and natural seawater.

Parameter	Treated wastewater	Natural seawater
pH	7.76	8.40
Conductivity	2.01 mS/cm	44.5 mS/cm
Total organic carbon (TOC)	3.62 mg/L	1.36 mg/L
Total carbon (TC)	18.74 mg/L	19.40 mg/L
Inorganic carbon (IC)	15.12 mg/L	18.04 mg/L
Total nitrogen (TN)	4.08 mg/L	1.91 mg/L
Mg	34.99 mg/kg	1198.14 mg/kg
Ca	20 mg/kg	390.56 mg/kg
S	39.90 mg/kg	904.31 mg/kg
Si	19.26 mg/kg	1.02 mg/kg

$$\text{Experimental moles} = V/V_0 \quad (2)$$

where V is the measured volume, V_0 is 24.45 L, and the gas volume is 1 mol at 1 atm and 298 K.

$$\text{Theoretical moles} = I \times t/n \times F \quad (3)$$

where I is the measured current, t is the time for gas collection, n is the stoichiometric number of electrons consumed in the electrode reaction ($n = 2$ for hydrogen production and $n = 4$ for oxygen production), and F is the Faraday constant.

3. Results and discussion

Hydrogen is produced from the electroreduction of water when the catholyte is neutral or basic, as shown in Equation (1) in Fig. 1, resulting in alkalization of the catholyte due to hydroxides as a by-product. On the other hand, acidification of the catholyte occurs from the synergetic effect of the proton flux from the BPM and inorganic precipitation at the cathode surface when low-grade water containing Mg^{2+} cations and BPM are used as the catholyte and separator, respectively [16]. Inorganic precipitation plays a role in capturing the hydroxides generated from the HER (Equation. (2) in Fig. 1), suppressing the increase in the pH of the catholyte. The proton flux generated from the WD of the BPM diffuses to the bulk catholyte through the open area of the BPM that is not in contact with the porous cathode, acidifying the catholyte [17]. The acidification continuously dissolves some inorganic deposits formed on the cathode, minimizing the growth rate of inorganic precipitates (Equation. (3) in Fig. 1). A portion of the proton flux is directly converted into hydrogen through an electron transfer reaction within the porous cathode (Equation. (4) in Fig. 1).

In this study, the acidification mechanism was applied to a low-grade water electrolyzer using treated wastewater as a catholyte. A certain amount of natural seawater (70 mL) was mixed with the treated wastewater (130 mL) because the concentration of Mg^{2+} ions in the treated wastewater was too low to induce acidification. For the control case, NaCl (0.5 M) was added to the treated wastewater to achieve a similar ionic conductivity. Fig. 2 shows the changes in pH and ionic conductivity of the catholyte over time at a constant current density (20 mA/cm^2) in the BPM-based electrolyzer (catholyte//BPM//0.5 M NaOH). When a mixture of treated wastewater and NaCl is used as the catholyte, the pH increases to 12 for operations longer than 100 h (Fig. 2a), implying that the HER driven by the electroreduction of water generates hydroxides. The continuous production of hydroxides reflects a linear increase in ionic conductivity (Fig. 2b). Although the proton generated in the BPM is provided to the catholyte, it is insufficient to completely compensate for the amount of hydroxides from the HER because only half of the total current within the BPM is carried by the protons. On the other hand, the mixture of treated wastewater and natural seawater shows stable acidification (~pH 3) during operation, which indicates that inorganic precipitation capturing hydroxides is an essential factor for acidification of the catholyte. This also indicates that the organic substances contained in the treated wastewater have a negligible effect on the acidification of the catholyte. The rate of increase in the ionic conductivity is slower than that in the control case, which can be ascribed to inorganic precipitation.

The significant variation in the pH of the catholyte had a direct effect on the E_c. The equilibrium potential (E_{eq}) of the HER driven by

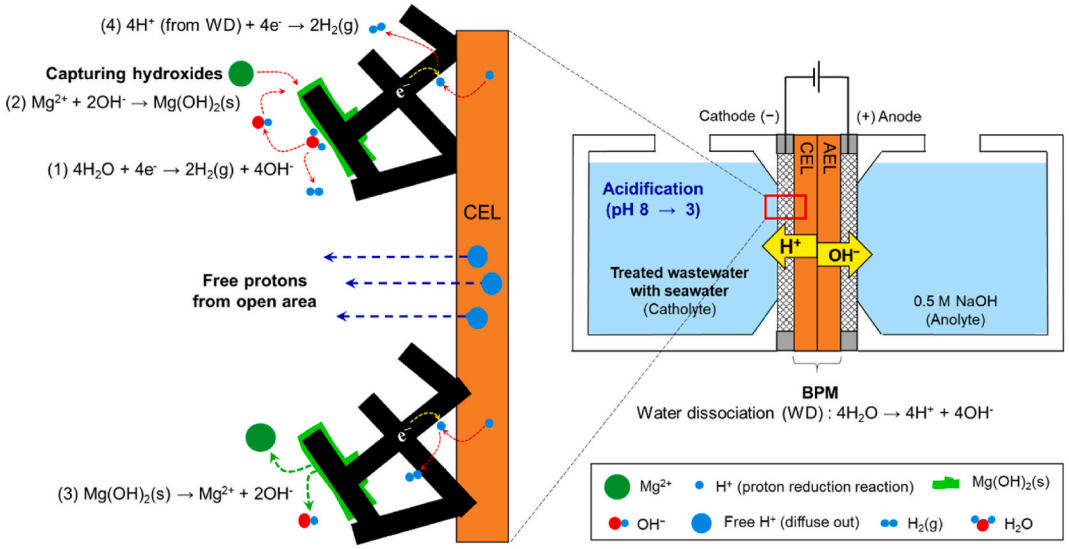

Fig. 1. Schematic of the low-grade water electrolysis based on acidification with an asymmetric electrolyte (treated wastewater added with natural seawater//BPM//0.5 M NaOH). CEL and AEL stand for cation exchange layer and anion exchange layer of the BPM, respectively. Protons and hydroxides generated from WD in BPM migrate in opposite directions due to electric field. Therefore, half of the total current is carried by protons and the other half by hydroxides within the BPM. The exposed area (7.065 cm^2) of the BPM with the electrolyte is the same as that of the porous electrodes. 0.5 M NaOH was used as an anolyte to suppress ClER. The open area through which free protons exit toward the bulk catholyte was created by cutting out a part of the porous cathode. The electrochemical equations provide quantitative information for understanding acidification.

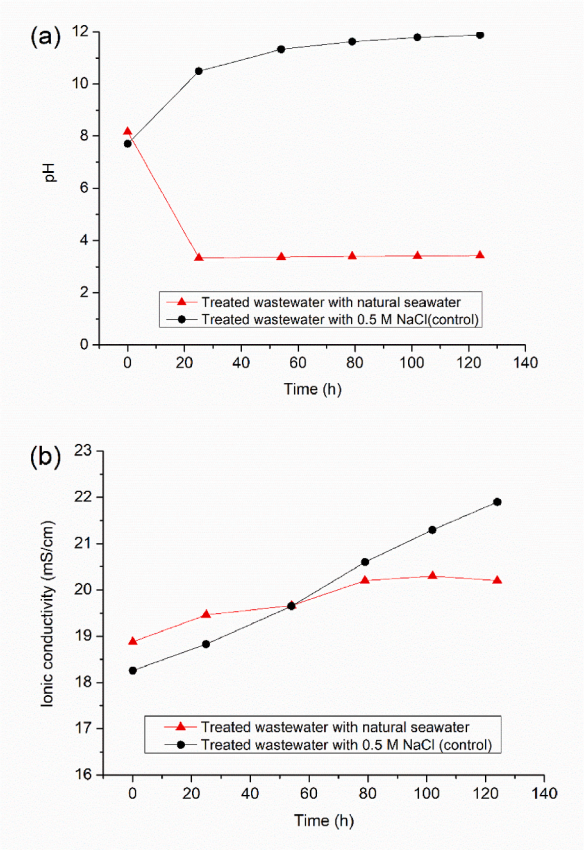

Fig. 2. Variations in (a) pH and (b) ionic conductivity of catholyte over time with two different catholytes (the treated wastewater with natural seawater or 0.5 M NaCl) in the BPM-based electrolyzer (catholyte//BPM//0.5 M NaOH). Note that 70 mL of natural seawater or 0.5 M NaCl solution was added to 130 mL of the treated wastewater. Geometrical current density was 20 mA/cm^2.

the water reduction reaction shifts negatively as the local pH at the cathode surface increases, following the Nerntian relationship [9, 21] in the standard hydrogen electrode scale.

$$E_{eq} = -0.059 \times pH \tag{4}$$

Acidification suppresses the negative shift of E_{eq} as the pH does not increase. Fig. 3 shows the changes in E_c when the treated wastewater with natural seawater or 0.5 M NaCl solution is used as the catholyte. The NaCl mixture shows a continuous negative shift for an operation longer than 100 h (Fig. 3a), as the catholyte became alkaline. Based on the initial E_c measured after 2 h of electrolysis, the increase rate (%) of E_c after 100 h was calculated using the following equation:

$$\text{increase rate } (\%) \text{ of Ec} = \frac{E_t - E_i}{E_t} \times 100 \tag{5}$$

The increase rate of E_c was 10% for the treated wastewater with NaCl solution, whereas the seawater mixture had $-$ 1 % of increase rate, indicating positive shift. The positive shift of E_c in the seawater mixture appeared at the beginning (~30 h), and the corresponding E_c was maintained over 100 h of operation. This indicates that acidification of the catholyte keeps the E_c stable, even though inorganic precipitates are formed at the surface of the cathode. The shifts in E_m (Fig. S2a) and E_a (Fig. S2b) are the same regardless of the catholyte, which means that the variations in the pH of the catholyte affect only the E_c. The change in E_c according to the pH change of the catholyte reflects the cell potential (E_{cell}), showing a positive shift of E_{cell} at the beginning for the treated wastewater with seawater (Fig. 3b). Both cases show a constant increase in E_{cell}, because the electrodes are susceptible to corrosion by the chloride ions. It is necessary to apply an electrocatalyst with high corrosion resistance to acidification-based low-grade water electrolysis.

Referring to the E_{eq} shift due to the pH change, ΔE_c between NaCl (0.5 M) and natural seawater is thermodynamically estimated to be 531 mV, which is considerably higher than the measured value (114 mV). This can be attributed to the larger overpotential for the HER owing to inorganic precipitates with a low conductivity (Fig. 4). The treated wastewater added with seawater contained more Mg^{2+} ions than the control case. Therefore, more inorganic precipitates are formed at the surface of the cathode (Figs. 4a–1) than in the NaCl mixture (Figs. 4b–1). In the control case, inorganic deposits are formed only on the fibers, which are the backbone of the porous structure (Figs. 4b–2), whereas in the seawater mixture, inorganic precipitates that block macropores are also formed (Figs. 4a–2).

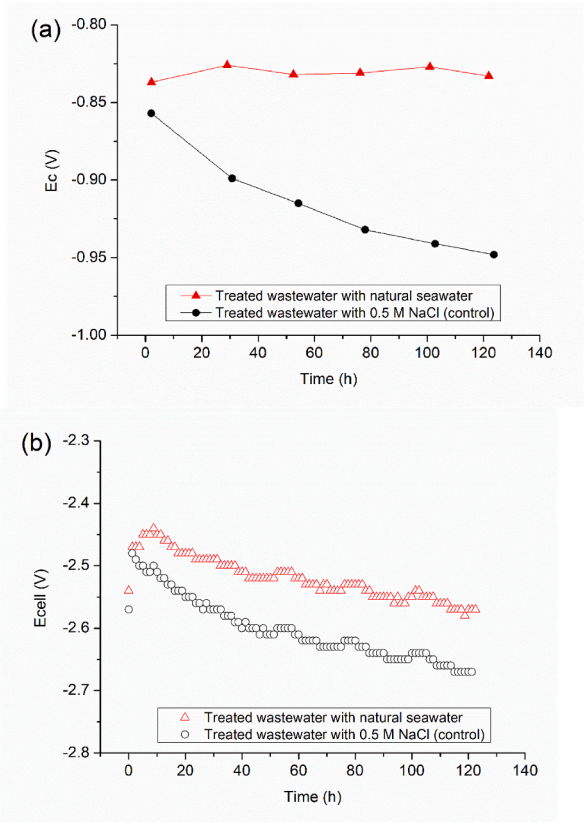

Fig. 3. Shifts of (a) cathode potential (E_c) and (b) cell potential (E_{cell}) for two different catholytes (the treated wastewater with natural seawater or 0.5 M NaCl solution) at 20 mA/cm^2 in the BPM-based electrolyzer (catholyte//BPM//0.5 M NaOH).

Nevertheless, the treated wastewater with seawater shows less negative E_c, indicating the important role of acidification in the performance of low-grade water electrolysis. The main composition of the inorganic precipitates was expected to be $Mg(OH)_2$ regardless of the type of catholyte, which is confirmed by EDS mapping analysis (Fig. S3), indicating that magnesium is the main element in the deposits. XRD analysis was also performed to confirm the chemical composition of the precipitates. The deposits of the treated wastewater with seawater are identified as $Mg(OH)_2$ (Fig. 4a–), whereas only the Ti peak is measured in the control case because of the very thin precipitates (Fig. 4b–).

Carbon and silicon are also identified, which are presumed to be derived from the organic matter contained in the treated wastewater. Previous studies have reported the co-precipitation of natural organic matter (NOM) with $Mg(OH)_2$ because of the favorable adsorption characteristics of $Mg(OH)_2$ (e.g., high surface area and positive surface charge) [22,23]. We measured the XPS spectra of the inorganic precipitates formed on the front side of the porous cathode to determine the relative abundances of the Si and C components (Fig. 5). Considering that some organic matter is contained in natural seawater (as shown in Table 1 earlier), the NOM concentration in the mixture of treated wastewater with natural seawater is higher than that in the control case. However, the Si2p peak of the inorganic precipitates is much larger in the control case (Fig. 5a and b), which can be attributed to the adsorption of more NOM owing to their negative charge from the alkalization of the catholyte. In the case of C1s (Fig. 5c and d), the mixture of seawater has one component at 284.4 eV associated with the C–C bond, whereas the control case shows two components at 284.4 eV and 289.5 eV associated with the C–C and C═O bonds, respectively. The pH of the catholyte appears to affect the chemical bonds of NOM co-precipitated with $Mg(OH)_2$. The Mg and Ca components are confirmed by the XPS spectra (Fig. S4). The control case shows a Ca2s peak as well as a Mg1s peak, whereas only the Mg 1s peak is measured in the effluent with natural seawater, indicating that acidification of the catholyte converts carbonate to CO_2 and inhibits the formation of calcium carbonate.

Acidification-based direct seawater electrolysis using natural seawater as a catholyte has been previously reported [17], where almost no inorganic precipitate was formed on the front side of the cathode. However, in this study, significant precipitates remain on the cathode despite the acidification of the catholyte. The co-precipitation of NOM with $Mg(OH)_2$ is assumed to be a factor that decreases the dissolution rate of inorganic precipitates.

On the back side of the porous cathode contacting the CEL of the BPM, relatively fewer inorganic deposits are formed regardless of the type of catholyte (Fig. 6a-1, 6b-1). This indicates that the proton flux generated from the WD of the BPM suppresses the formation of inorganic deposits on the back side of the porous cathode. For the treated wastewater with seawater, although the center of the porous cathode is covered with inorganic deposits (Figs. 6a–2), the macropores are not blocked by the precipitates, unlike on the front

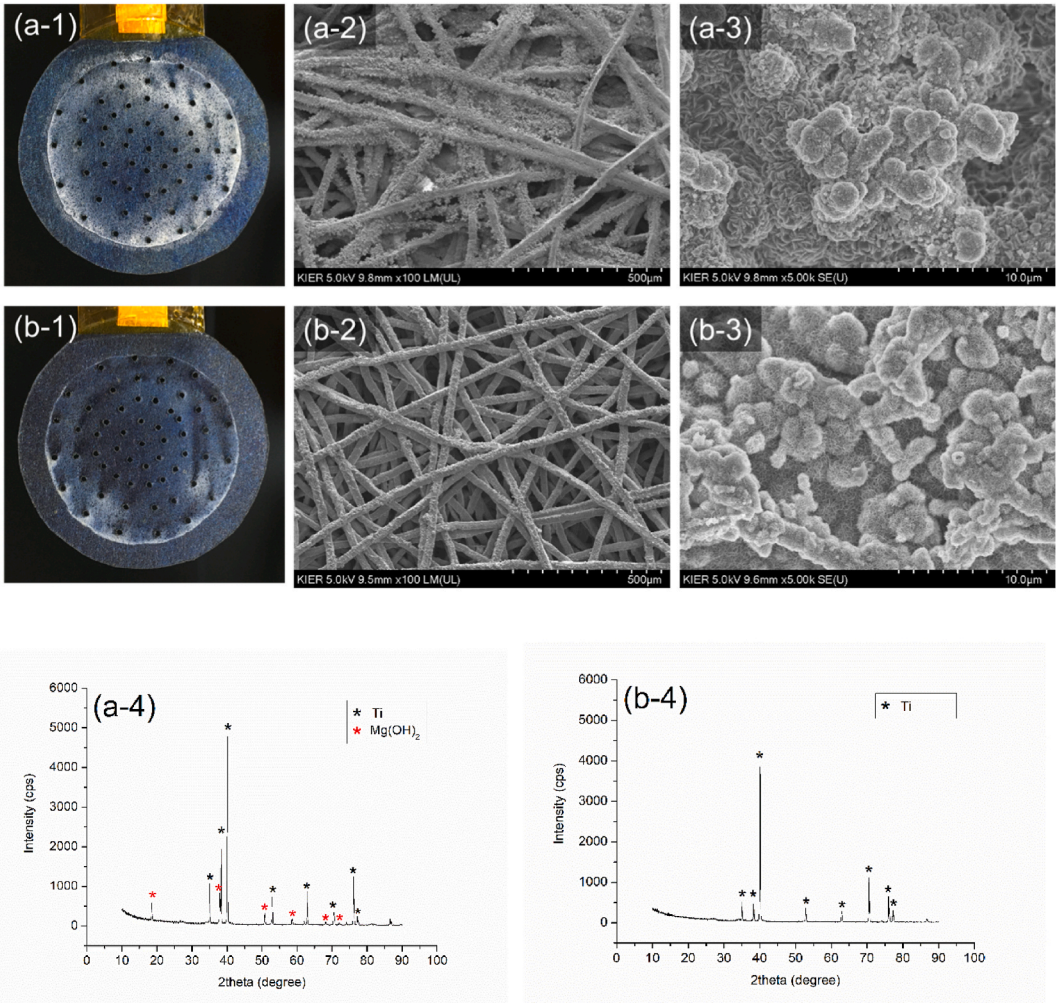

Fig. 4. (a-1, b-1) Photographs, (a-2,3 and b-2,3) SEM images, and (a-4, b-4) XRD data of inorganic precipitates formed on the front (facing the catholyte) sides of the porous cathodes for two different catholytes (the treated wastewater added with (a) natural seawater or (b) 0.5 M NaCl) after operation at 20 mA/cm^2 for 100 h.

side. At the edge (Figs. 6a–3), it is confirmed that a very small amount of inorganic precipitate is formed with a low atomic percentage (~1 %) of Mg (Figs. 6a–4). The control case also shows the absence of noticeable precipitates on the back side (Figs. 6b–3, 4), except for a small amount of inorganic deposits in the central part (Figs. 6b–2). There is a high possibility that the porous cathode in the middle part does not completely come into contact with the BPM because of the structure of the water electrolyzer in this study, by which more inorganic deposits could be formed at the center region of the back side. The zero-gap structure between the BPM and porous cathode can be fully achieved by applying a rigid mesh through which the catholyte can flow to evenly press the porous cathode. This will be conducted as a follow-up study in the near future.

Acidification serves to keep the thickness of the inorganic precipitates thin by dissolving some of the deposits, which is confirmed by the variation in the concentration of Mg^{2+} ions (Fig. 7a). Mg^{2+} ions in the control case are completely removed because of alkalization of the catholyte, whereas 80 % of the initial concentration of Mg^{2+} ions remains when the treated wastewater added with seawater is used as the catholyte. The acidification converts IC such as carbonates and bicarbonates to gaseous carbon dioxide (Fig. 7b). Therefore, the concentration of IC in the treated wastewater with natural seawater is almost zero after 100 h of electrolysis, whereas the control case (0.5 M NaCl) shows a two-fold increase, resulting from accelerating acid dissociation reactions of dissolved carbon dioxide by alkalization. However, TOC and TN increase to similar concentrations, although the pH of the two cases is dramatically different. The AEL in the BPM is susceptible to corrosive environments [24]. The nucleophile (OH^- or Cl^-) can result in the chemical decomposition of the ammonium group (acting as a functional group) of AEL in the BPM. Hence, it is necessary to analyze change in functional group of AEL as a function of electrolysis time in future studies. Because the large-scale low-grade water electrolysis stack produces hydrogen while flowing the electrolyte, the TOC and TN of the treated wastewater discharged from the stack are expected to be almost the same as those of the inflow water, minimizing the environmental impact on nearby discharge areas.

Fig. 8 shows the Faradaic efficiency of H_2 over time with the two different catholytes. At the beginning of the low-grade water

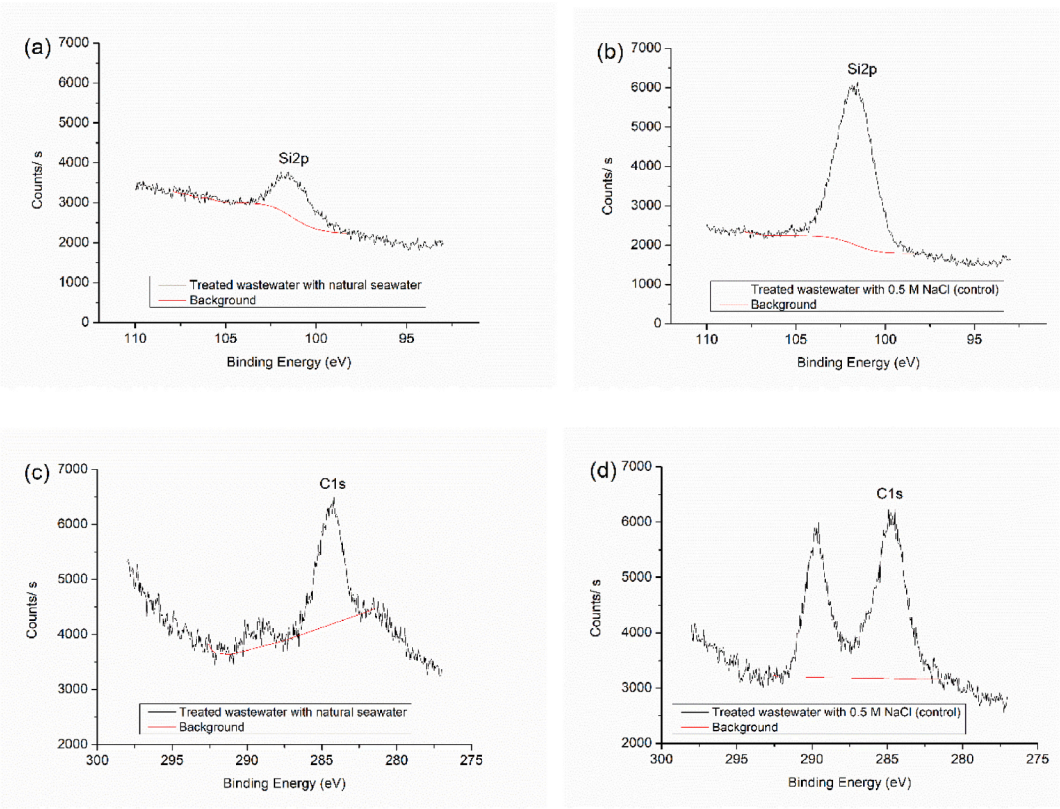

Fig. 5. High-resolution XPS spectra of (a, b) Si2p and (c, d) C1s of the inorganic precipitates formed on the front side of porous cathode depending on the catholytes (the treated wastewater added with natural seawater or 0.5 M NaCl).

electrolysis, the efficiency (~73 %) of the seawater mixture is lower than that of the NaCl mixture. However, it continues to increase and reaches 90 %, which is similar to the NaCl mixture despite inorganic precipitates forming on the cathode surface and pores. Owing to the characteristics of the chamber-type electrolyzer, the hydrogen gas does not directly escape into the collection pack, remaining in the form of bubbles on the chamber wall, which limits the accurate measurement of the hydrogen volume. This can be solved by applying a stack structure, in which the electrolyte is forced to flow using a pump. The energy consumption for the seawater mixture in the system is 6.7 kWh/Nm^3. Although it consumes more electric power as compared to that of state-of-the-art water electrolysis (4.2–5.0 kWh/m^3) [25], the development of electrocatalysts with high corrosion resistance can significantly improve its performance. Hydrogen production based on membrane area is 0.076 Nm^3/m^2•hr for seawater mixture.

Author contribution statement

Ji-Hyung Han: Conceived and designed the experiments; Performed the experiments; Analyzed and interpreted the data; Contributed reagents, materials, analysis tools or data; Wrote the paper.

Jeongwook Bae, Joohyun Lim: Performed the experiments.

Eunjin Jwa, Joo-Youn Nam, Kyo Sik Hwang, Namjo Jeong: Analyzed and interpreted the data.

Jiyeon Choi, Hanki Kim, Youn-Cheul Jeung: Contributed reagents, materials, analysis tools or data.

4. Conclusions

This study demonstrates the direct electrolysis of treated wastewater discharged from a sewage treatment plant to produce hydrogen based on the acidification of the catholyte induced by the synergetic effect between the proton flux from the BPM and inorganic precipitation. Treated wastewater containing some natural seawater has a certain amount of Mg^{2+} ions, which leads to inorganic precipitation at the surface of the cathode, and thus the acidification of the catholyte. Although the amount of inorganic deposits formed on the cathode surface in the mixture of treated wastewater and seawater was larger than that in the treated wastewater with NaCl solution (control case), acidification of the seawater mixture allowed the initial cathode potential to be maintained over 100 h, showing a stable performance. This contrasts with the control case, where the cathode potential continuously increased owing to the alkalization. It was also confirmed that less organic matter was adsorbed to the inorganic deposits under acidic conditions. Because some sewage treatment plants are located along the coast, direct electrolysis of treated wastewater with seawater

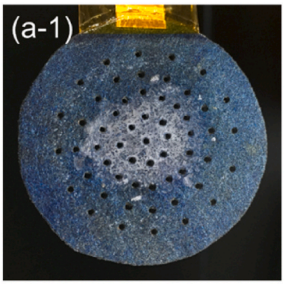

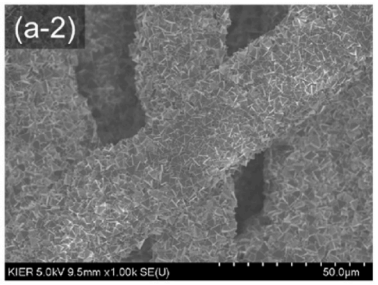

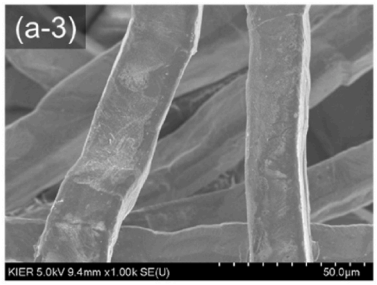

Treated wastewater added with natural seawater

(a-4)

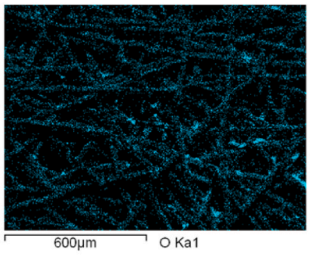

Element	Weight%	Atomic%
O K	25.64	53.30
Mg K	1.05	1.44
Ti K	60.61	42.09
Ru L	1.59	0.52
Sn L	6.79	1.90
Ir M	4.32	0.75
Totals	100.00	

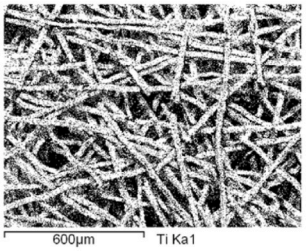

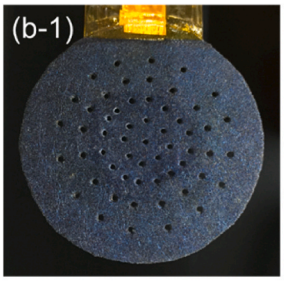

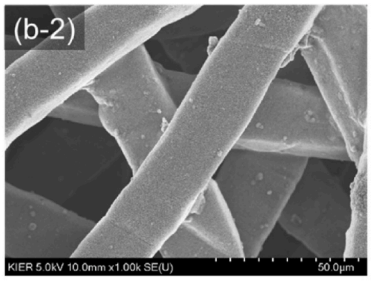

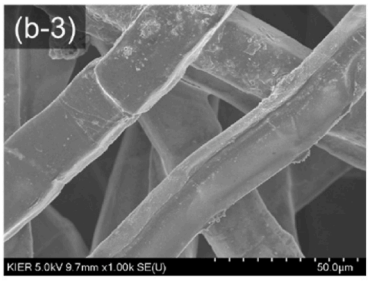

Treated wastewater added with 0.5 M NaCl

(b-4)

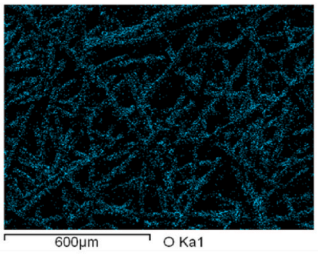

Element	Weight%	Atomic%
O K	21.83	47.19
Mg K	0.23	0.33
P K	0.15	0.17
Ti K	69.25	50.01
Ru L	1.16	0.40
Sn L	5.10	1.49
Ir M	2.27	0.41
Totals	100.00	

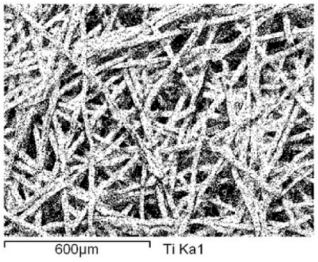

(caption on next page)

Fig. 6. (a-1, b-1) Photographs and SEM images of (a-2, b-2) the center and (a-3, b-3) edge of the back (facing the BPM) sides of the porous cathodes for two different catholytes (the treated wastewater added with (a) natural seawater or (b) 0.5 M NaCl) after operation at 20 mA/cm^2 for 100 h. (a-4, b-4) EDS mapping and element table of inorganic precipitates formed on the edge part.

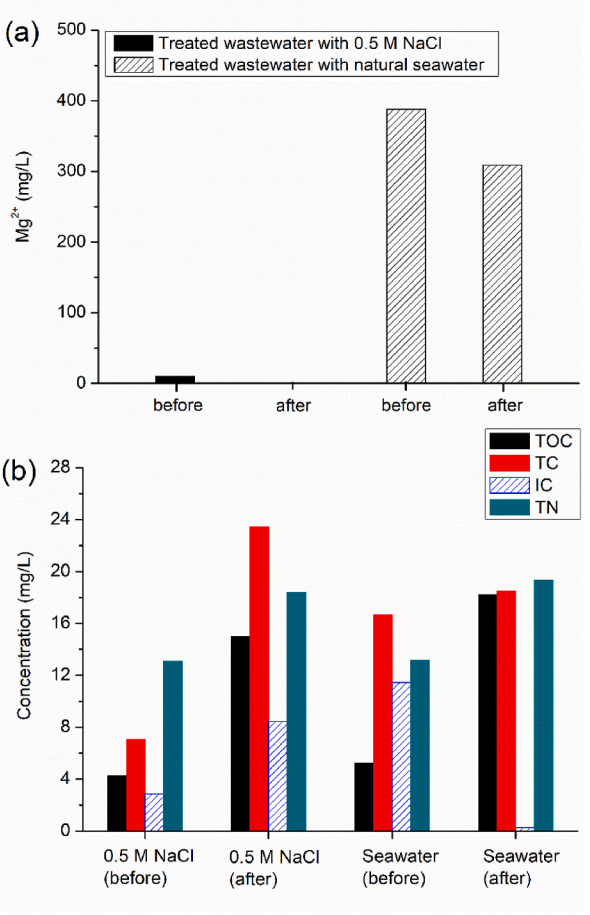

Fig. 7. Concentrations of (a) Mg^{2+} ions and (b) TOC, TC, IC, and TN in two different catholytes (the treated wastewater added with 0.5 M NaCl or natural seawater) before and after 100 h of operation at 20 mA/cm^2.

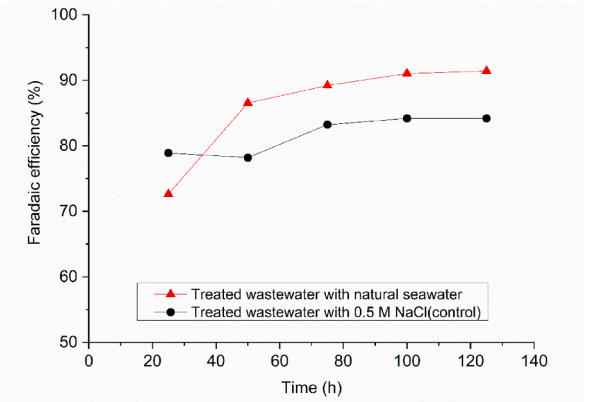

Fig. 8. Variations in the Faradaic efficiency for H_2 production over time with two different catholytes (the treated wastewater with natural seawater or 0.5 M NaCl). Geometrical current density was 20 mA/cm^2.

can be a promising technology to achieve stable hydrogen production with low electricity consumption due to acidification. In addition, considering that treated wastewater is directly discharged into the ocean, direct electrolysis of low-grade water can be implemented as a water reuse technology to enhance water resilience and contribute to the circular economy of water resources.

Data availability statement

Data will be made available on request.

Declaration of competing interest

The authors declare that they have no known competing financial interests or personal relationships that could have appeared to influence the work reported in this paper.

Acknowledgments

This work was supported by the National R&D Program through the National Research Foundation of Korea (NRF) funded by the Ministry of Science and ICT (No. 2022M3H4A4097522), a National Research Foundation of Korea (NRF) grant funded by the Korean government (MSIT) (No. NRF-2021R1F1A1061943), and the framework of the international cooperation program managed by the National Research Foundation of Korea (NRF-2023K2A9A2A22000124). We would like to thank Mr. Sung Don Kim for helping us collect the treated wastewater and seawater.

Appendix A. Supplementary data

Supplementary data to this article can be found online at https://doi.org/10.1016/j.heliyon.2023.e20629.

References

[1] L. Ma, S. Sui, Y. Zhai, Investigations on high performance proton exchange membrane water electrolyzer, Int. J. Hydrog. Energy 34 (2) (2009) 678–684, https://doi.org/10.1016/j.ijhydene.2008.11.022.
[2] K. Zeng, D. Zhang, Recent progress in alkaline water electrolysis for hydrogen production and applications, Prog. Energy Combust. Sci. 36 (3) (2010) 307–326, https://doi.org/10.1016/j.pecs.2009.11.002.
[3] R.R. Beswick, A.M. Oliveira, Y. Yan, Does the green hydrogen economy have a water problem? ACS Energy Lett. 6 (9) (2021) 3167–3169, https://doi.org/10.1021/acsenergylett.1c01375.
[4] L.F. Greenlee, D.F. Lawler, B.D. Freeman, B. Marrot, P. Moulin, Reverse osmosis desalination: water sources, technology, and today's challenges, Water Res. 43 (9) (2009) 2317–2348, https://doi.org/10.1016/j.watres.2009.03.010.
[5] E.R. Jones, M.T.H. van Vliet, M. Qadir, M.F.P. Bierkens, Country-level and gridded estimates of wastewater production, collection, treatment and reuse, Earth Syst. Sci. Data 13 (2) (2021) 237–254, https://doi.org/10.5194/essd-13-237-2021.
[6] UN, UN World Water Development Report, The Untapped Resource, Wastewater, 2017.
[7] J. Du, T.D. Waite, J. Feng, Y. Lei, W. Tang, Coupled electrochemical methods for nitrogen and phosphorus recovery from wastewater: a review, Environ. Chem. Lett. 21 (2) (2023) 885–909, https://doi.org/10.1007/s10311-023-01561-x.
[8] J. Du, T.D. Waite, P.M. Biesheuvel, W. Tang, Recent advances and prospects in electrochemical coupling technologies for metal recovery from water, J. Hazard Mater. 442 (2023), 130023, https://doi.org/10.1016/j.jhazmat.2022.130023.
[9] J.E. Bennett, Electrodes for generation of hydrogen and oxygen from seawater, Int. J. Hydrog. Energy 5 (4) (1980) 401–408, https://doi.org/10.1016/0360-3199(80)90021-X.
[10] D.W. Kirk, A.E. Ledas, Precipitate formation during sea water electrolysis, Int. J. Hydrog. Energy 7 (12) (1982) 925–932, https://doi.org/10.1016/0360-3199(82)90160-4.
[11] W. Tong, M. Forster, F. Dionigi, S. Dresp, R. Sadeghi Erami, P. Strasser, A.J. Cowan, P. Farràs, Electrolysis of low-grade and saline surface water, Nat. Energy 5 (5) (2020) 367–377, https://doi.org/10.1038/s41560-020-0550-8.
[12] M. Patel, W.-H. Park, A. Ray, J. Kim, J.-H. Lee, Photoelectrocatalytic sea water splitting using Kirkendall diffusion grown functional Co3O4 film, Sol. Energy Mater. Sol. Cells 171 (2017) 267–274, https://doi.org/10.1016/j.solmat.2017.06.058.
[13] M.M. Ayyub, M. Chhetri, U. Gupta, A. Roy, C.N.R. Rao, Photochemical and photoelectrochemical hydrogen generation by splitting seawater, Chem. Eur J. 24 (69) (2018) 18455–18462, https://doi.org/10.1002/chem.201804119.
[14] X. Li, W. Xing, T. Hu, K. Luo, J. Wang, W. Tang, Recent advances in transition-metal phosphide electrocatalysts: synthetic approach, improvement strategies and environmental applications, Coord. Chem. Rev. 473 (2022), 214811, https://doi.org/10.1016/j.ccr.2022.214811.
[15] X. Lu, J. Pan, E. Lovell, T.H. Tan, Y.H. Ng, R. Amal, A sea-change: manganese doped nickel/nickel oxide electrocatalysts for hydrogen generation from seawater, Energy Environ. Sci. 11 (7) (2018) 1898–1910, https://doi.org/10.1039/C8EE00976G.
[16] J.-H. Han, E. Jwa, H. Lee, E.J. Kim, J.-Y. Nam, K.S. Hwang, N. Jeong, J. Choi, H. Kim, Y.-C. Jeung, T.D. Chung, Direct seawater electrolysis via synergistic acidification by inorganic precipitation and proton flux from bipolar membrane, Chem. Eng. J. 429 (2022), 132383, https://doi.org/10.1016/j.cej.2021.132383.
[17] J.-H. Han, Exploring the interface of porous cathode/bipolar membrane for mitigation of inorganic precipitates in direct seawater electrolysis, ChemSusChem 15 (11) (2022), e202200372, https://doi.org/10.1002/cssc.202200372.
[18] K. Vijayaraghavan, D. Ahmad, R. Lesa, Electrolytic treatment of beer brewery wastewater, Ind. Eng. Chem. Res. 45 (20) (2006) 6854–6859, https://doi.org/10.1021/ie0604371.
[19] J.O.M. Bockris, Environmental Chemistry, Springer New York, NY1977.
[20] F. Dionigi, T. Reier, Z. Pawolek, M. Gliech, P. Strasser, Design criteria, operating conditions, and nickel–iron hydroxide catalyst materials for selective seawater electrolysis, ChemSusChem 9 (9) (2016) 962–972, https://doi.org/10.1002/cssc.201501581.
[21] T. Shinagawa, K. Takanabe, Towards versatile and sustainable hydrogen production through electrocatalytic water splitting: electrolyte engineering, ChemSusChem 10 (7) (2017) 1318–1336, https://doi.org/10.1002/cssc.201601583.

[22] M. AzadiAghdam, M. Park, I.J. Lopez-Prieto, A. Achilli, S.A. Snyder, J. Farrell, Pretreatment for water reuse using fluidized bed crystallization, J. Water Process Eng. 35 (2020), 101226, https://doi.org/10.1016/j.jwpe.2020.101226.
[23] C.G. Russell, D.F. Lawler, G.E. Speitel Jr., NOM coprecipitation with solids formed during softening, J. AWWA (Am. Water Works Assoc.) 101 (4) (2009) 112–124, https://doi.org/10.1002/j.1551-8833.2009.tb09879.x.
[24] R.A. Tufa, M.A. Blommaert, D. Chanda, Q. Li, D.A. Vermaas, D. Aili, Bipolar membrane and interface materials for electrochemical energy systems, ACS Appl. Energy Mater. 4 (8) (2021) 7419–7439, https://doi.org/10.1021/acsaem.1c01140.
[25] N. Tenhumberg, K. Büker, Ecological and economic evaluation of hydrogen production by different water electrolysis technologies, Chem. Ing. Tech. 92 (10) (2020) 1586–1595, https://doi.org/10.1002/cite.202000090.